The effect of dendritic pendants on the folding of amphiphilic copolymers via supramolecular interactions

The Effect of Dendritic Pendants on the Folding of Amphiphilic Copolymers Via Supramolecular Interactions

This manuscript is dedicated to Professor Mitsuo Sawamoto's outstanding achievements in polymer chemistry and recognizes his recent retirement from 40 years of exceptional service to Kyoto University.

Gijs M. ter Huurne, Ghislaine Vantomme, Bart W. L. van den Bersselaar, Bala N. S. Thota, Ilja K. Voets, Anja R. A. Palmans, E. W. Meijer

Institute for Complex Molecular Systems, Laboratory of Macromolecular and Organic Chemistry, Eindhoven University of Technology, P.O. Box 513, 5600 MB, Eindhoven, The Netherlands
Correspondence to: A. R. A. Palmans (E-mail: a.palmans@tue.nl); I. K. Voets (E-mail: i.voets@tue.nl); E. W. Meijer (E-mail: e.w.meijer@tue.nl)

Received 20 July 2018; Accepted 9 August 2018; published online 4 October 2018
DOI: 10.1002/pola.29223

ABSTRACT: The supramolecular folding of amphiphilic heterograft copolymers equipped with dendritic pendants is investigated using a combination of proton nuclear magnetic resonance (^{1}H NMR) spectroscopy, small-angle X-ray scattering, and circular dichroism spectroscopy. Hereto, the linear poly(ethylene glycol) pendants normally used to convey water compatibility are partially substituted with branched analogues. For one set of copolymers, second-generation polyglycerol dendrons are directly attached to the polymer backbone, while for the other a hydrophilic linker is placed in between. The results show that the branching of the hydrophilic pendants affects the local structure of the folded copolymer but does not influence the overall conformation and single-chain character of the folded copolymers in solution. All copolymers fold into 4–5 nm single-chain polymeric nanoparticles with a very compact spherical morphology, independent of the dendritic content of the copolymer. Intriguingly, the incorporation of the dendritic pendants affects the formation of a structured interior even at low incorporation ratios. © 2018 Wiley Periodicals, Inc. J. Polym. Sci., Part A: Polym. Chem. **2019**, *57*, 411–421

KEYWORDS: amphiphilic; folding; dendritic; dendronized; polymer; single-chain polymeric nanoparticle; supramolecular

INTRODUCTION Nature has evolved an amazing arsenal of molecular machinery to sustain life. One of its major components is proteins, fulfilling a wide variety of functions in an incredibly efficient and selective way. Intriguingly, the distinct function of a protein is directly related to its precisely controlled three-dimensional structure.[1–3] By studying the delicate structure–function relation observed in proteins, some of Nature's design principles have been elucidated.[3,4] By applying these design principles, new interesting synthetic materials have been developed.[5–8] The close relationship between the structure and function of proteins has been a major source of inspiration to the field of macromolecular science,[9] resulting in many elegant examples in which rudimentary structural features of proteins have been mimicked. For example, the hydrophobic pocket of enzymes has been successfully mimicked by incorporating catalytically active groups in the hydrophobic domains of star polymers, micelles, and vesicles.[10–19] In addition, macromolecular architectures with an extremely well-defined 3D morphology were developed in the form of dendrimers and helical polymers, such as foldamers.[20–29] However, the excellent structural control and properties provided by such perfectly defined synthetic structures, comes at the cost of a relatively demanding synthesis.

Inspired by Mitsuo Sawamoto's controlled polymer synthesis, a similar extent of structural control with simplified synthetic architectures was obtained and key elements of dendrimers were incorporated into amphiphiles and polymers. The unique 3D architecture of such dendritic amphiphiles has been used to construct self-assembled nanostructures with diverse morphologies.[30–32] Similarly, the conformation of polymers could be controlled via the attachment of dendritic pendants. The synthesis of such dendronized polymers is well established and their characteristics are actively studied, both experimentally and theoretically. Depending on the dendritic content and design of the dendrons, polymers can be highly stretched, collapsed, or everything in between.[33–42] Similar to polymers grafted with a high density of long linear pendants, such as bottle brush polymers, dendronized polymers are stretched by ample incorporation of sufficiently large dendrons.[43,44] However, modeling studies do not yet agree on the effect of the pendant's degree of branching on the stretching of the polymers. While some studies

Additional supporting information may be found in the online version of this article.

suggest that dendritic pendants, compared to linear pendants, induce stretching of a polymer chain at lower degrees of incorporation or via the use of smaller pendants, others suggest no influence of the degree of branching.[45–48] Furthermore, surfaces, such as membranes, are expected to become less rigid, and thus more bendable, when grafted with more branched architectures.[49,50]

Nowadays, a popular method to control the conformation of synthetic polymers is the so-called single-chain polymeric nanoparticles (SCPNs) approach. Here, individual polymers are intramolecularly collapsed into nanoparticles by means of covalent, dynamic covalent, or supramolecular crosslinks.[51–53] Whereas a variety of hydrogen bonding groups have been applied in organic media to collapse polymers,[54–61] only few are capable of inducing the collapse and subsequent folding in water.[62–66] Especially, the inherent ability of benzene-1,-3,5-tricarboxamides (BTAs) to self-assemble into helical supramolecular polymers—stabilized by threefold hydrogen bonding—proved to be a versatile way to control the conformation of a single polymer chain in solution.[67–69]

Inspired by Israelachvili's theory on the self-assembly of surfactants, in which he showed that the shape of a micelle is directly related to the geometry of an individual surfactant, we investigate whether the curved nature of dendritic pendants can be used to promote the intramolecular folding of supramolecular amphiphilic heterograft copolymer into spherical nanoparticles.[70] Hereto, the linear poly(ethylene glycol) pendants normally used to convey water compatibility are partially substituted with branched analogues, more specifically with second-generation polyglycerol dendrons.[67–69,71,72] These dendritic units are well soluble in aqueous media and are highly biocompatible.[73–76] Two sets of copolymers were synthesized to study the effect of the dendron incorporation (Fig. 1). In set A, various amounts of the dendron were directly attached to the polymer backbone. In set B, the dendrons were attached via a hydrophilic linker. A combination of small-angle X-ray scattering (SAXS) experiments and circular dichroism (CD) spectroscopy measurements reveals that both dendritic architectures form around 4-nm-sized spherical single-chain polymer nanoparticles, but also that the incorporation of dendritic pendants reduces the degree to which a structured interior is formed.

RESULTS

Synthesis and Characterization of a Second-Generation Dendron

Two different derivatives of a second-generation polyglycerol dendron were synthesized. In set A, the dendron (**8**) is directly attached to the polymer backbone and in set B, the dendron (**18**) is attached via a hydrophilic hexa(ethylene glycol) linker (Scheme 1). Both of the dendrons were synthesized in an iterative approach, starting with the reaction between two equivalents of racemic solketal (**1**) with one equivalent of methallyl dichloride (**2**).[73] Next, the double bond in the resulting first-generation dendron (**3**) was converted into an alcohol group (**4**) via a subsequent ozonolysis and reduction step. Two equivalents of this product (**4**) were reacted with methallyl dichloride (**2**) to obtain a second-generation polyglycerol dendron (**5**). By performing another subsequent ozonolysis and reduction step, a second-generation alcohol functionalized dendron (**6**) was obtained. The newly introduced alcohol group was activated using mesyl chloride and directly transformed into an azide group (**7**). The final product, Prot-G_2-NH_2 (**8**), was obtained by a reduction of the azide using hydrogen gas in an overall yield of 24% over six steps.

For the other protected second-generation polyglycerol amine (**18**), a hydrophilic spacer was prepared. Hereto, hexa(ethylene glycol) was protected on one side using *tert*-butyl bromoacetate (**10**). Afterward, the remaining free alcohol group (**11**) was activated in a reaction with tosyl chloride (**12**). The activated alcohol group was purified and directly reacted with potassium phthalimide (**14**) forming compound **15**. After the removal of the protecting *tert*-butyloxycarbonyl group using trifluoroacetic acid, the linker (**16**) was coupled to the protected second-generation polyglycerol amine (**8**) using *o*-(benzotriazol-1-yl)-*N*,*N*,*N*′,*N*′-tetramethyluronium tetrafluoroborate as the coupling reagent. The final product, Prot-G_2-HEG-NH_2 (**18**), was obtained after removal of the phthalimide group with hydrazine in an overall yield of 13%. Pentafluorophenyl acrylate (**19**) was polymerized using reversible addition–fragmentation chain transfer (RAFT) polymerization (Scheme 2). After removal of the RAFT-end group, the poly(pentafluorophenyl acrylate) homopolymer (**P2**) was grafted with amine-functionalized groups in a sequential fashion (Scheme 2). For the different copolymer sets, A and B, two large batches of **P2** were separately functionalized with the hydrophobic *n*-dodecylamine and the structuring BTA-C_{11}-NH_2, in the optimal ratio as found in prior research (15 and 5 mol %, respectively).[69] One of these two large batches was split into four smaller batches and functionalized with various amounts of Prot-G_2-NH_2 (**8**), while the other large batch was split into four and subsequently functionalized with Prot-G_2-HEG-NH_2 (**18**). This was done to ensure that the copolymers within set A contain an equal number of *n*-dodecylamine and BTA-C_{11}-NH_2 units, as well as all the copolymers within set B. All these functionalization steps were performed with the diols of the dendron protected with acetonide groups to prevent a side reaction between dendron's alcohol groups and the copolymer's activated esters. Interestingly, the maximal incorporation of Prot-G_2-NH_2 (**8**) proved to be limited to approximately 30 mol %. Apparently, the remaining reactive centers of the copolymer (50 mol %) are no longer accessible at these compositions and conditions.[77] This already suggests a significant crowding effect induced by the sterically demanding dendrons. Prot-G_2-HEG-NH_2 (**18**) could be incorporated to larger extents. As a result of the limited accessibility of the remaining reactive ester groups, a huge excess of hydrophilic Jeffamine M-1000 (~320 equivalents) was required to fully functionalize all the dendronized precursor polymers.

For all the copolymers, the conversion of each sequential post-functionalization step was monitored using ^{19}F NMR

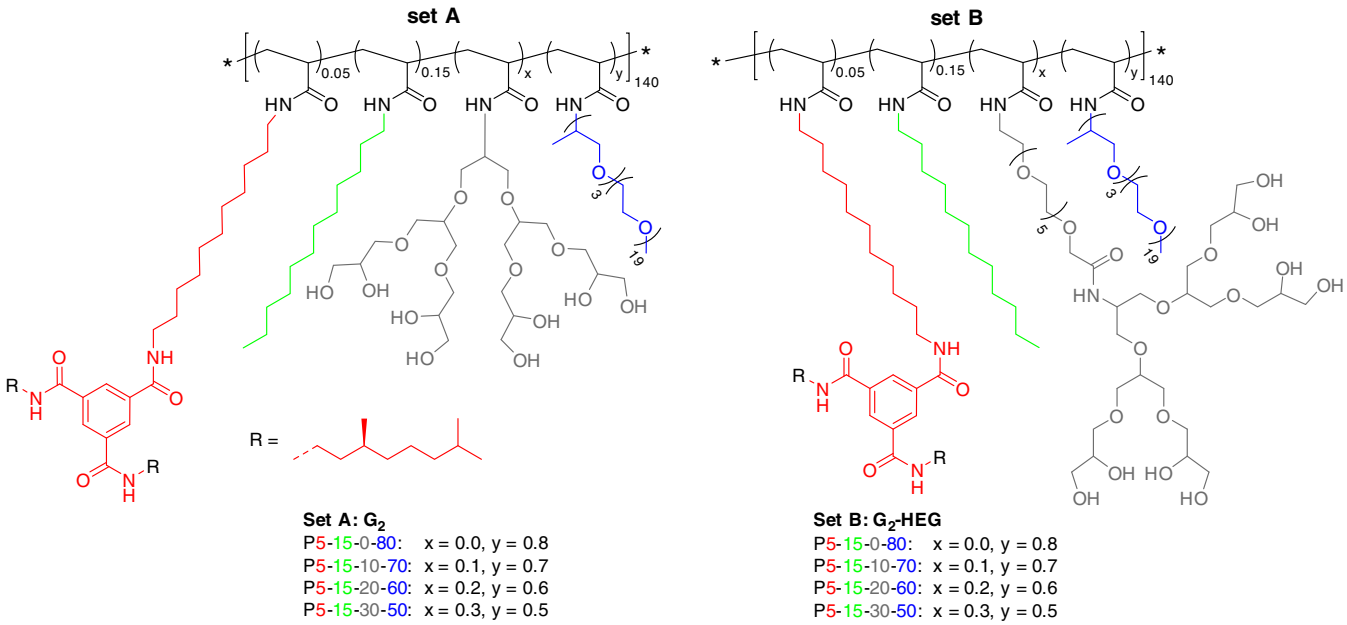

FIGURE 1 Chemical structures of the amphiphilic heterograft copolymer containing 15 mol % dodecylamine, 5 mol % BTA-C_{11}-NH_2, and various amounts of dendritic (x) and Jeffamine M-1000 (y) pendants. In set A, the dendrons are directly attached to the polymer backbone. In set B, the dendrons are attached via a hydrophilic linker.

spectroscopy by comparing the signals corresponding to the released pentafluorophenol to those of the precursor polymers.[69,78,79] The ^{19}F NMR spectra confirmed that the sequential incorporation of the different amines roughly matched with the feed ratios. The copolymers were purified via a consecutive dialysis against tetrahydrofuran and methanol, followed by precipitation in cold *n*-pentane. The final poly(acrylamide) copolymers with a degree of polymerization of around 140, showed values for the number-average molecular weight (M_n) ranging from 24.5 to 28.2 kg mol^{-1} and dispersity (Đ) varying between 1.15 and 1.24 (Table 1).

The fully functionalized, acetonide-protected copolymers were characterized by proton nuclear magnetic resonance (^{1}H NMR) spectroscopy in $CDCl_3$. For the copolymers of set A, with the protected dendrons directly attached to the backbone, ^{1}H NMR spectra with broadened signals were obtained (Fig. S1). Interestingly, for the copolymers of set B, containing Prot-G_2-HEG, splitting of the signals corresponding to the outermost glycerol moieties was observed. This indicates that the protected second-generation polyglycerol dendrons are significantly more mobile in chloroform, when attached to the copolymer backbone via a hydrophilic linker.

The synthesis of the dendronized copolymers was completed by deprotection of the dendritic pendants using a dilute HCl solution (Scheme 2). This reaction was monitored using ^{1}H NMR spectroscopy, by following the disappearance of the signals corresponding to the protecting groups (Figs. S1 and S2). Upon reaching full conversion, the copolymers were purified via a dialysis against methanol, followed by precipitation in cold *n*-pentane.

Sample Preparation Procedure

In previous works, the sample preparation procedure proved to be crucial to the folding of amphiphilic copolymers.[69,80] In this work, dissolving of the copolymers, in deionized water, was facilitated by 1 h of sonication. Afterward, the samples were cooled to room temperature, left standing overnight, and filtered using a 100 nm PVDF filter.

Overall Conformations of the Dendronized Copolymers

SAXS experiments were performed to get insight into the relationship between the composition of the deprotected dendronized copolymers and their conformation in solution. The scattering profiles obtained for all the copolymers were featureless curves leveling off at low q values, which is typical for small polymeric nanoparticles in solution [Fig. 2(A,B)]. The radii of gyration and weight-average macromolecular weights were determined via the shape-independent Guinier analysis (Table 2). The fitting range was set such that the maximum q to be included is $\leq 1.3 \cdot R_G^{-1}$. From the intensity of these plateaus at low q values, the weight-average molecular weight (M_W) of the nanoparticles in solution was estimated (Table 2).

For the copolymers of set A, with the dendritic pendants directly attached to the polymer backbone, the intensity of the plateau at low q values was observed to decrease as a function of the dendritic content [Fig. 2(A)]. This indicates that mass of the copolymers in solution becomes lower upon increasing the G_2 content. Such a gradual reduction of the copolymer's molecular weight, as a function of the dendritic content, is expected since the dendrons are introduced as the direct substitute for the heavier Jeffamine M-1000 pendants (M = 695.4 and ~1050 g mol^{-1}, respectively). These theoretically calculated values proved to match closely with the

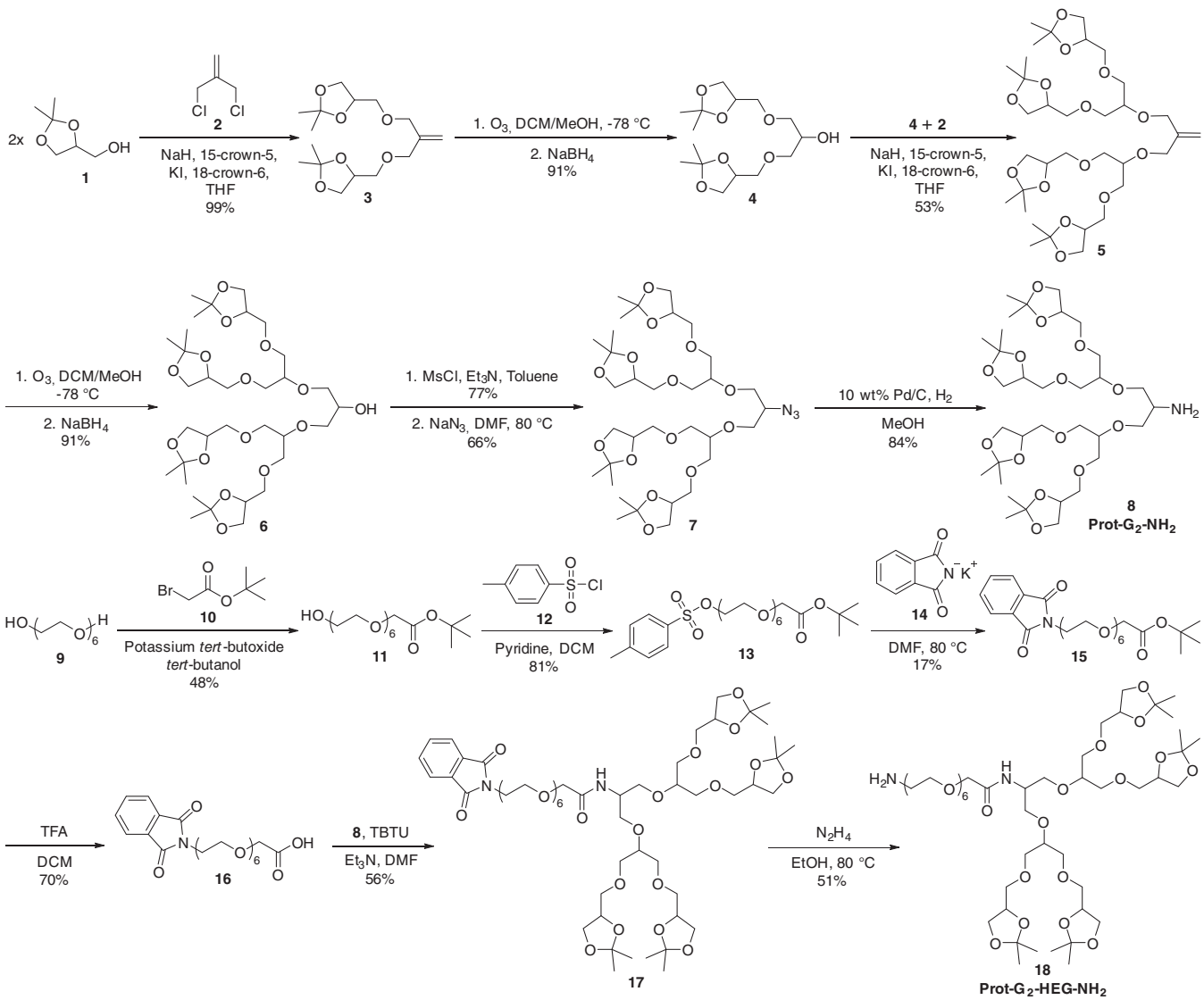

SCHEME 1 Iterative synthesis of a protected second-generation polyglycerol dendron amine without (Prot-G_2-NH_2, **8**) and with a hexa(ethylene glycol) linker (Prot-G_2-HEG-NH_2, **18**).

molecular masses determined with SAXS (Table 2). This suggests that all these copolymers are present as SCPNs, regardless of their composition. Because all the scattering curves can be successfully fitted with a polymer excluded volume model, we conclude that the folded copolymers adopt a globular conformation in solution. In addition, this analysis provides insight into the compactness of the formed nanoparticles via the excluded volume parameter from the Flory mean field theory (ν) (Table 2).[81,82] A system's ν value provides information about the effective solvent quality and is thus related to the compactness of the system. The lower the ν value, the more compact the conformation of the homopolymer coil. For polymers in a bad solvent, a theoretical lower limit of 0.33 is to be expected. Our obtained ν values are slightly lower than this lower limit, which is attributed to the structured interior of the nanoparticles. Based on this insight, in combination with the Guinier analysis, we conclude that all copolymers fold into very compact globular SCPNs with a radius of gyration (R_G) of approximately 4 nm (Table 2).

For the copolymers grafted with the G_2-HEG dendrons, set B, the intensity of the plateau at low q values appears to be virtually independent of the copolymer composition [Fig. 2(B)]. This indicates that these copolymers in solution form nanoparticles with a comparable molecular weight. Here, the similar molecular weights of G_2-HEG-NH_2 and Jeffamine M-1000 (1016.6 and ~1050 g mol^{-1}, respectively) cause changes in the ratio between these two pendants to have a negligible effect on the copolymer's molecular weight. Again, the theoretically expected masses are in close agreement with the values obtained with SAXS (Table 2). Regardless of the exact composition, the G_2-HEG-containing copolymers also form 4–5 nm SCPNs with a very compact spherical morphology.

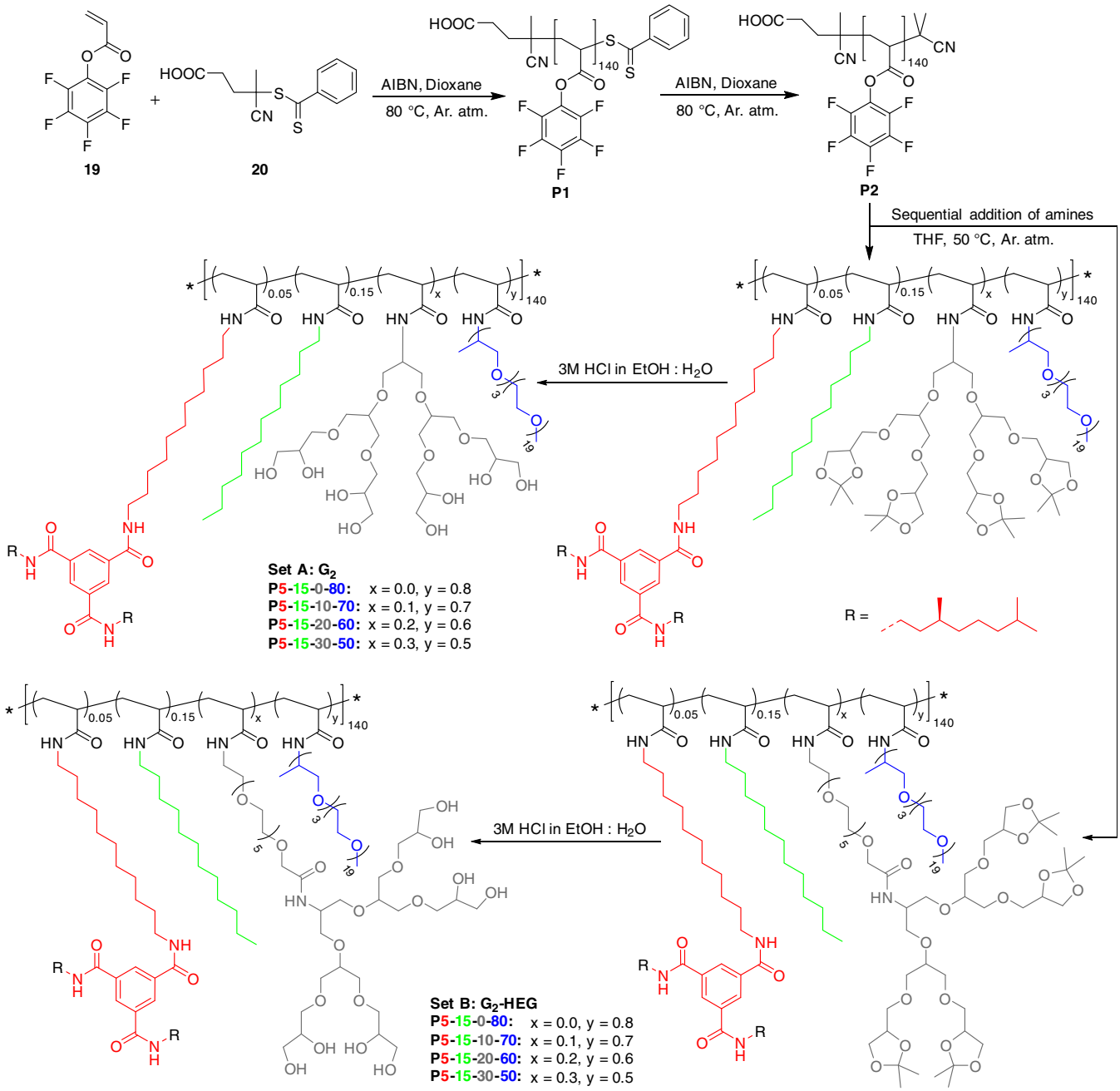

SCHEME 2 Synthesis and sequential postfunctionalization of a poly(pentafluorophenyl acrylate) homopolymer with 15 mol % dodecylamine, 5 mol % BTA-C_{11}-NH_2, and various amount of dendritic (x), and Jeffamine M-1000 (y) pendants. In set A, the dendrons are directly attached to the polymer backbone. In set B, the dendrons are attached via a hydrophilic linker. Subsequently, the dendritic pendants were deprotected using acid.

Internal Structure of the Copolymers

As described above, the scattering curves obtained are similar at intermediate q values. Therefore, similar R_G and ν values are extracted by fitting of the curves, indicating that the overall conformation of the dendronized copolymers is not significantly affected by the incorporation of the branched pendants. From the high q regime of the scattering curves, information about the local structure of the SCPNs can be obtained. At a low degree of dendron incorporation (10 mol %), the normalized scattering curves overlap over the entire q range [Fig. 3(A)]. This suggests that, at this composition, the conformation of the G_2- and G_2-HEG-containing copolymers is effectively the same at all observed length scales. However, upon increasing the dendron content to 20 or 30 mol %, a slightly different decay can be discerned between q = 1 and 4 nm^{-1} [Fig. 3(B)]. This different decay indicates that the folded copolymers possess an additional 1–2-nm-sized structure. Most likely, this additional local structure is related to a local

TABLE 1 Copolymer Composition, Number-Average Molecular Weight (M_n), and Dispersity (Đ) of the Acetonide Protected Copolymers of Sets A and B

	BTA (mol %)[a]	Dodecyl (mol %)[a]	Dendron (mol %)[a]	Jeffamine M-1000 (mol %)[a]	$M_{n,\ SEC}$ (kg mol^{-1})[b]	Đ[b]
Prot-G_2						
P5-15-0-80	5	15	0	80	28.2	1.24
P5-15-10-70	5	15	10	70	26.7	1.18
P5-15-20-60	5	15	20	60	26.2	1.17
P5-15-30-50	5	15	30	50	25.6	1.16
Prot-G_2-HEG						
P5-15-0-80	5	15	0	80	28.2	1.24
P5-15-10-70	5	15	10	70	26.7	1.18
P5-15-20-60	5	15	20	60	26.2	1.17
P5-15-30-50	5	15	30	50	25.6	1.16

[a] Based on the feed ratio.

[b] Determined with SEC in DMF, with respect to a poly(ethylene glycol) standard, using the copolymers with the protected dendritic pendants.

increase of the copolymer's cross-sectional diameter induced by the bulky nature of the dendritic pendants.[83]

Folding of the Dendronized Copolymers

Chiral BTA grafts fold a polymer backbone into a nanoparticle via the formation of helical, hydrogen-bond-based assemblies with a preferred handedness. The presence of such structured domains within the nanoparticles can be monitored with CD spectroscopy. A negative CD effect is indicative for the formation of left-handed helical BTA assemblies.[84] In addition, the shape of the CD effect provides information on the conformation of the hydrogen-bonded amides of the BTAs in the self-assembled state, whereas the magnitude of the signal is proportional to the fraction of BTA that is helically assembled. For all the copolymers, comprising approximately the same BTA and *n*-dodecyl content (5 and 10 mol %, respectively), a negative CD effect was observed with an identical shape. This indicates that all the copolymers contain structured left-handed self-assembled domains in which the amides of the BTAs adopt the same conformation. Importantly, the two slightly different copolymers from sets A and B, comprising without of only BTAs and linear hydrophilic grafts, have a similar CD effect with a molar CD ($\Delta\varepsilon$) of around -25 M^{-1} cm^{-1} [Fig. 4(A,B)]. This value is in close agreement with those obtained in prior research.[85] However, the incorporation of the dendritic grafts leads to a significant drop in the magnitude of the CD effect. The most pronounced decrease in CD effect is observed for the incorporation of the initial 10 mol %, independent of the architecture of the branched graft. Upon tripling the dendritic content of G_2, the magnitude of the CD effect slightly reduces [Fig. 4(A), $\Delta\varepsilon$ = -16–18 M^{-1} cm^{-1}]. Furthermore, the temperature dependence of the CD effect is in agreement with prior research, and thus not influenced by the dendritic grafts.[69] On the other hand, copolymers containing various amounts of G_2-HEG (10–30 mol %) have the exact same CD effect ($\Delta\varepsilon$ = -13 M^{-1} cm^{-1}), independent of their dendritic content [Fig. 4(B)]. Although replacing 10 mol % of Jeffamine M-1000 for dendrons suffices to induce

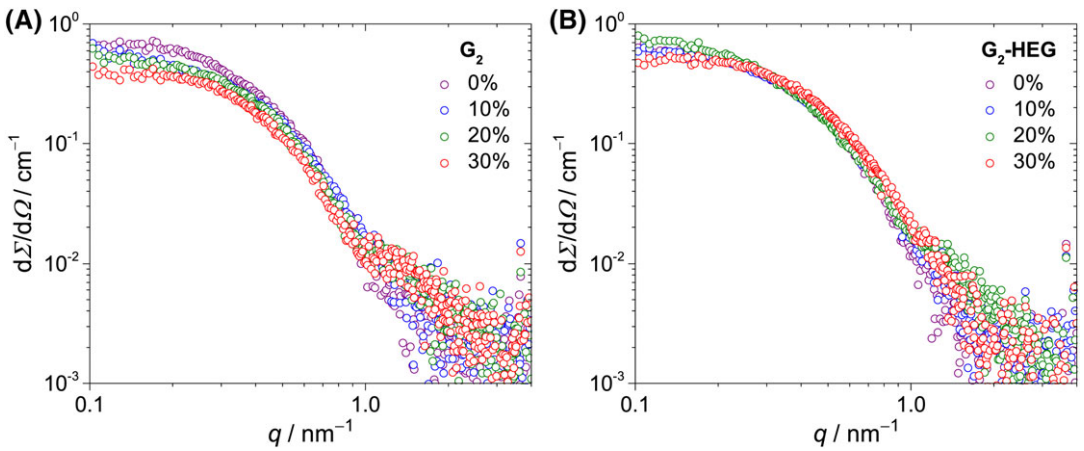

FIGURE 2 Comparison of the SAXS curves for **P5-15-x-y** ($c_{polymer}$ = 5 mg mL^{-1} in water, T = 20 °C) as a function of the incorporation of: (A) G_2; (B) G_2-HEG.

TABLE 2 Overview of the Effect of the Copolymer Composition on the Radius of Gyration (R_G), Absolute Scattering Intensity at $q \rightarrow 0$ (I_0), Excluded Volume Parameter (ν), Weight-Average Molecular Weight (M_w), and the Aggregation Number (N_{agg})

Dendron (mol %)	R_G (nm)[a]	I_0 (cm^{-1})[a]	ν (–)[b]	$M_{w,\ SAXS}$ (kDa)	$M_{w,\ calc.}$ (kDa)[c]	N_{agg} (–)[d]
Set A: G_2						
0	4.4	0.7780	0.34	159.2	164.9	1.02
10	4.3	0.5742	0.24	124.2	148.6	0.84
20	4.1	0.5424	0.23	117.3	139.0	0.84
30	3.8	0.4401	0.21	123.1	129.6	0.95
Set B: G_2-HEG						
0	4.4	0.647	0.23	139.9	162.2	0.86
10	4.5	0.648	0.27	181.2	155.2	1.17
20	4.9	0.810	0.40	226.6	149.5	1.52
30	3.8	0.624	0.26	174.5	144.0	1.21

[a] Determined using the Guinier analysis, error in $R_G < 5\%$.
[b] Determined using the polymer excluded volume model.
[c] $M_{w,\ calc.} = [(M_{BTA} \cdot n_{BTA}) + (M_{dodecyl} \cdot n_{dodecyl}) + (M_{dendron} \cdot n_{dendron}) + (M_{Jeffamine\ M\text{-}1000} \cdot n_{Jeffamine\ M\text{-}1000}) + M_{endgroups}] \cdot Đ$.
[d] $N_{agg} = M_{w,\ SAXS}/M_{w,\ calc.}$

an immediate decrease in $|\Delta\varepsilon|$, a higher incorporation of the dendrons does not lead to additional reduction in BTA self-assembly. To further elucidate the origin of the trends observed in the CD effect, the protected dendronized copolymers were studied. Surprisingly, all the Prot-G_2-containing copolymers have a similar CD effect with a magnitude similar to that of the copolymer only comprising without of linear hydrophilic pendants [Fig. 5(A)]. This shows that the BTAs self-assemble to a similar extent, irrespective of the copolymer's Prot-G_2 content. Apparently, the sterically demanding nature of the protected G_2 dendrons does not significantly affect the self-assembly of the BTA grafts. For set B, the CD effect observed for the copolymers with a 0 and 30 mol % G_2-HEG incorporation has a magnitude similar to the G_2-containing copolymers [Fig. 5(B)]. Remarkably, the two other polymers (10 and 20 mol % G_2-HEG) have a lower CD effect. These results indicate that a change in the polarity of the end groups has a large effect on the formation of a supramolecular internal structure, but the shape of the dendrons does not.

DISCUSSION

The supramolecular folding of amphiphilic heterograft copolymers equipped with dendritic pendants shows similarities but also pronounced differences compared to their counterparts that only comprise without of Jeffamine M-1000 side chains. By eye, all the dendronized copolymers seem to be better soluble in aqueous solutions than the copolymers containing only linear hydrophilic pendants. Presumably, the branched nature of the dendrons induces more disorder in the polymer brush, making them easier to solubilize.

SAXS measurements were performed on the amphiphilic heterograft copolymers. The masses of the copolymers, determined using SAXS in solution, proved to be in close agreement with the theoretically expected values. Therefore, it is concluded that all the copolymers fold into single-chain polymer nanoparticles, regardless of their exact composition. Interestingly, the SAXS experiments indicate that a

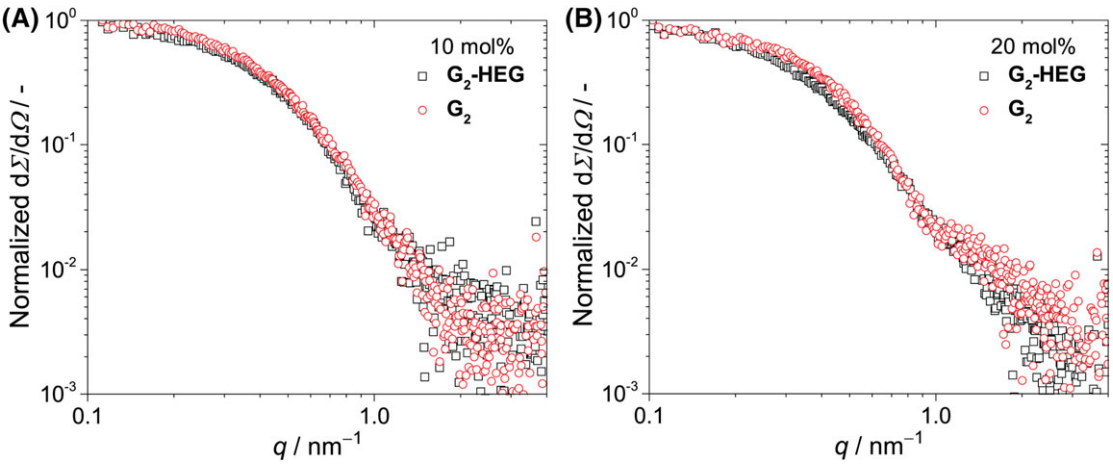

FIGURE 3 Normalized SAXS curves ($c_{polymer}$ = 5 mg mL^{-1} in water, T = 20 °C) at a G_2 and G_2-HEG incorporation of: (A) 10 mol %; (B) 20 mol %.

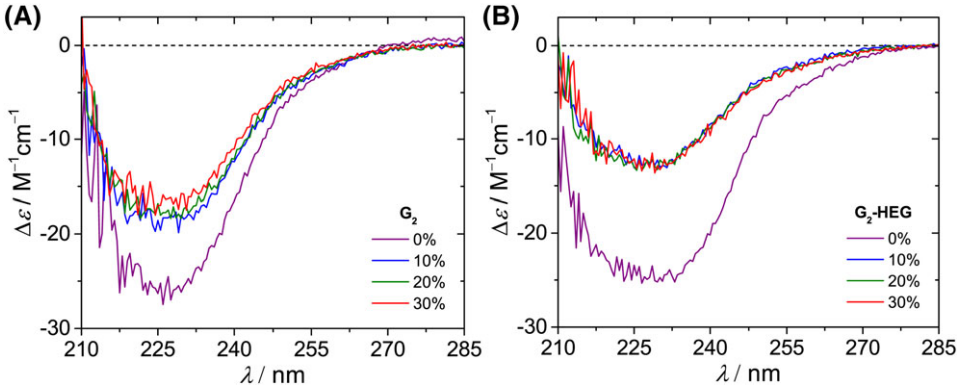

FIGURE 4 Comparison of the molar CD spectra obtained for **P5-15-x-y** (c_{BTA} = 50 μM in water, T = 20 °C) as a function of the incorporation of: (A) G_2; (B) G_2-HEG.

20–30 mol % incorporation of the dendritic architectures does introduce an additional 1–2-nm-sized structure in the folded nanoparticles. This structure is attributed to a local increase of the copolymer's cross-sectional diameter due to the attachment of bulky dendritic pendants to the polymer backbone. These observations suggest that the dendrons are more densely packed around the polymer backbone than the linear counterparts. Surprisingly though, this evidential impact of geometry of the hydrophilic pendants on the polymer conformation remains localized, and is thus not translated into an overall stretching of the copolymer. As a result, all copolymers adopt a compact spherical conformation with a radius of gyration of approximately 4–5 nm, independent of the dendritic content of the copolymer. These sizes are slightly smaller than what has been observed before for similar supramolecular amphiphilic heterograft copolymers.[67–69] However, the work presented here uses X-rays for the small-angle scattering experiments, whereas in previous studies neutrons were applied. The contrast between water and poly(ethylene glycol) is larger in neutron scattering experiments, which makes a PEG-based corona more visible. As a result, the radii of gyration can be slightly larger when determined via SANS. Based on the SAXS experiments, we conclude that the curved and bulky architecture of these dendritic pendants does not provide a significant benefit to the intramolecular folding of supramolecular amphiphilic heterograft copolymer, in comparison to linear branches (Fig. 6).

Further evidence for this statement is obtained by CD spectroscopy experiments. These measurements were performed to investigate how the balance between branched and linear hydrophilic pendants influences the self-assembly of the supramolecular grafts. Interestingly, a substantial drop in the magnitude of $|\Delta\varepsilon|$ from 25 to around 12–15 M^{-1} cm^{-1} is observed for all dendronized copolymers. This indicates that the deprotected dendrons reduce the degree of helical order between the BTA pendants. Interestingly, CD spectroscopy indicates that the folding of the dendronized copolymers is only slightly dependent on the copolymer's G_2 content, and completely unaffected by increases in G_2-HEG content. Intriguingly, in both cases the BTA self-assembly seems to be limited to a fixed extent. Presumably, the incorporation of the dendrons forces the nanoparticle to adopt a compact conformation in which the self-assembly of the supramolecular grafts is limited to a specific degree.

To elucidate the origin of these surprising results, the protected dendronized copolymers were studied using CD spectroscopy. Intriguingly, the magnitude of the CD effect is independent of the copolymer's Prot-G_2 content. This indicates that the sterically

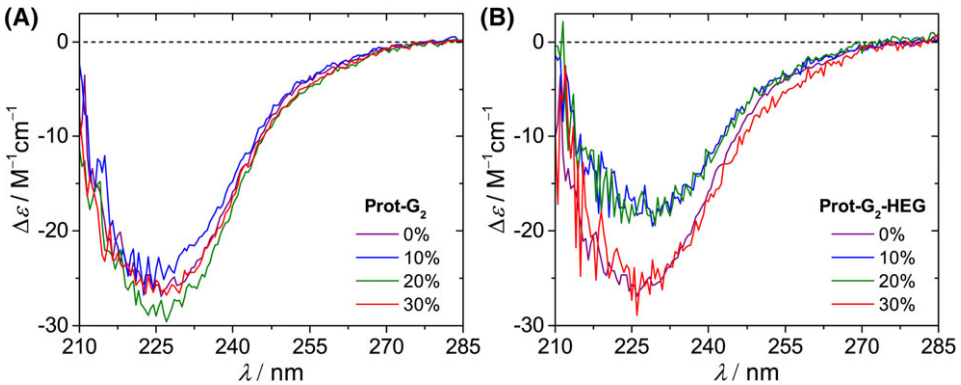

FIGURE 5 Comparison of the molar CD spectra obtained for **P5-15-x-y** (c_{BTA} = 50 μM in water, T = 20 °C) as a function of the incorporation of: (A) Prot-G_2; (B) Prot-G_2-HEG.

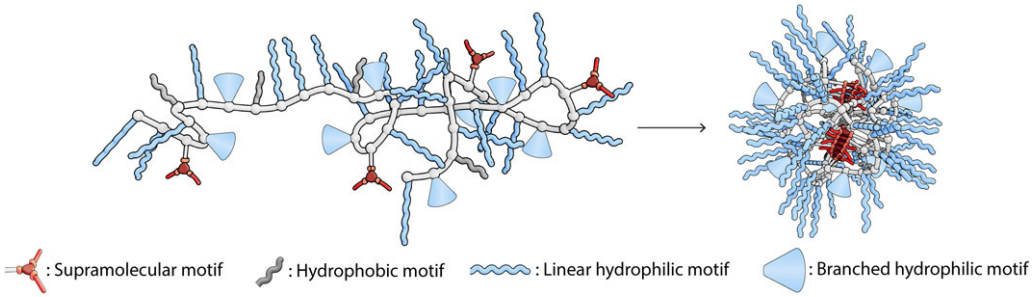

FIGURE 6 Schematic representation of the folding of supramolecular amphiphilic heterograft copolymers containing dendritic pendants.

demanding nature of Prot-G_2 does not significantly affect the self-assembly of the BTA grafts. However, the incorporation of Prot-G_2-HEG displays a surprising trend. The CD effect observed for the copolymers with a 0 and 30 mol % Prot-G_2-HEG incorporation has a magnitude similar to the Prot-G_2-containing copolymers. However, the magnitude of the CD effect in the two other polymers (10 and 20 mol % Prot-G_2-HEG) is lower. We attribute this to degradation processes in these copolymers, as the deprotected G_2-HEG-containing copolymers proved to be prone to crosslinking over time. This unstable nature of the deprotected G_2-HEG-containing copolymers might also be the reason for the larger deviations in the numbers obtained from the SAXS experiments, compared to the deprotected G_2-containing copolymers (Table 2). Assuming that the geometry of the dendrons remains similar upon deprotection, we conclude that the different trends observed in CD spectroscopy are strongly related to the change of the dendron's end groups. Presumably, the free alcohol groups of the deprotected dendrons are interfering with the stabilizing hydrogen bonds of the BTA stacks, just like the addition of isopropanol has proven to do.[67] This would suggest that at least a part of the dendritic pendants must be in close proximity of the hydrophobic BTAs.

Prior research has shown that folding of amphiphilic heterograft copolymer using supramolecular interactions results in nanoparticles containing multiple, structured domains.[65,68] It could be that, in resemblance to self-assembled supramolecular systems in water, a certain fraction of these domains are strongly associated while others are weakly bound.[86] These weakly associated domains could be more accessible and thus easier to disrupt. Here, the fixed hydrophobic content of the amphiphilic heterograft copolymers could mean that the ratio between the different domains is approximately constant. Therefore, only a fixed fraction of the BTAs can be disassembled by the OH end groups of the dendritic pendants, explaining the surprising CD results.

Furthermore, Sawamoto and coworkers recently studied the folding of comparable amphiphilic heterograft copolymers using ^{1}H NMR spectroscopy.[87] They reported that in order to facilitate the formation of stable nanoparticles, a part of the hydrophilic grafts is incorporated in the hydrophobic core. SCPNs formed by copolymers with a higher hydrophobic content proved to have a larger fraction of the hydrophilic side chains present in the hydrophobic core. Therefore, it was concluded that the fraction of the hydrophilic pendants that is internalized in the core is directly related to the copolymer's hydrophobic content. Extending these insights to our dendronized amphiphilic heterograft copolymers, with a constant hydrophobic content, implies that an approximately constant fraction of the hydrophilic grafts is internalized in the hydrophobic core of the SCPNs. This constant fraction of internalized hydrophilic pendants can interfere with the BTA stacks, while the rest is present on the exterior of the SCPN. As a result, an increase in the dendritic content of the copolymers does not lead to a further destabilization of its structured internal core.

CONCLUSIONS

Inspired by the amazing science of Mitsuo Sawamoto, we investigated the folding of dendronized amphiphilic heterograft copolymers using a combination of ^{1}H NMR spectroscopy, CD spectroscopy, and SAXS. Hereto, the typically used linear poly(ethylene glycol) derivative was partially substituted with branched hydrophilic analogues. For one set, the dendrons were directly attached to the polymer backbone, while for the other, a hydrophilic linker was placed in between. The results show that although the geometry of the hydrophilic pendants impacts the polymer conformation on a local level, all the copolymers adopt a compact spherical conformation with a radius of gyration of approximately 4–5 nm. Because this behavior is independent of the dendritic content of the copolymer, we conclude that the curved and bulky architecture of these dendritic pendants does not provide a distinct difference to the intramolecular folding of supramolecular amphiphilic heterograft copolymer, in comparison to linear branches. Intriguingly, even the slightest incorporation of a dendritic pendant limits the formation of a structured interior to a fixed extent. Most likely, this is due to the polar end groups of the dendrons interfering with the self-assembly of supramolecular pendants. This research will benefit the further understanding of the folding and structure of amphiphilic heterograft copolymers in solution via supramolecular interactions. It therefore aids in the overall goal to obtain protein-like structural control over synthetic macromolecular structures. It is our pleasure to dedicate this article to Mitsuo Sawamoto for his continuous support of original polymer chemistry and well-defined polymers by living polymerization, a technique so important for the work presented here.

ACKNOWLEDGMENTS

The authors would like to thank Rainer Haag (FU Berlin) for stimulating discussions. This work is financed by the Dutch Ministry of Education, Culture and Science (Gravity program 024.001.035). G.V. is grateful for financial support from the Netherlands Organization for Scientific Research (NWO – VENI grant 722.017.003). The ICMS Animation Studio (Eindhoven University of Technology) is acknowledged for providing the artwork.

REFERENCES

1 C. B. Anfinsen, *Science* **1973**, *181*, 223.

2 C. M. Dobson, *Nature* **2003**, *426*, 884.

3 M. I. Sadowski, D. T. Jones, *Curr. Opin. Struct. Biol.* **2009**, *19*, 357.

4 B. J. G. E. Pieters, M. B. van Eldijk, R. J. M. Nolte, J. Mecinović, *Chem. Soc. Rev.* **2016**, *45*, 24.

5 S. Tadepalli, J. M. Slocik, M. K. Gupta, R. R. Naik, S. Singamaneni, *Chem. Rev.* **2017**, *117*, 12705.

6 L. Montero De Espinosa, W. Meesorn, D. Moatsou, C. Weder, *Chem. Rev.* **2017**, *117*, 12851.

7 Y. Liu, K. He, G. Chen, W. R. Leow, X. Chen, *Chem. Rev.* **2017**, *117*, 12893.

8 C. Zhang, D. A. M. Ii, J. C. Grunlan, *Adv. Mater.* **2016**, *28*, 1.

9 J. F. Lutz, J. M. Lehn, E. W. Meijer, K. Matyjaszewski, *Nat. Rev. Mater.* **2016**, *1*, 16024.

10 A. Lu, R. K. O'Reilly, *Curr. Opin. Biotechnol.* **2013**, *24*, 639.

11 G. Polymeropoulos, G. Zapsas, K. Ntetsikas, P. Bilalis, Y. Gnanou, N. Hadjichristidis, *Macromolecules* **2017**, *50*, 1253.

12 V. Rodionov, H. Gao, S. Scroggins, D. A. Unruh, A.-J. Avestro, J. M. J. Fréchet, *J. Am. Chem. Soc.* **2010**, *132*, 2570.

13 K. Matyjaszewski, *Macromolecules* **2012**, *45*, 4015.

14 T. Terashima, *Polym. J.* **2014**, *46*, 664.

15 X. Fan, Z. Li, X. J. Loh, *Polym. Chem.* **2016**, *7*, 5898.

16 J. M. Ren, T. G. McKenzie, Q. Fu, E. H. H. Wong, J. Xu, Z. An, S. Shanmugam, T. P. Davis, C. Boyer, G. G. Qiao, *Chem. Rev.* **2016**, *116*, 6743.

17 Y. Zhao, F. Sakai, L. Su, Y. Liu, K. Wei, G. Chen, M. Jiang, *Adv. Mater.* **2013**, *25*, 5215.

18 M. T. De Martino, L. K. E. A. Abdelmohsen, F. P. J. T. Rutjes, J. C. M. van Hest, *Beilstein J. Org. Chem.* **2018**, *14*, 716.

19 B. C. Buddingh, J. C. M. Van Hest, *Acc. Chem. Res.* **2017**, *50*, 769.

20 J. M. Frechet, *Science* **1994**, *263*, 1710.

21 A. W. Bosman, H. M. Janssen, E. W. Meijer, *Chem. Rev.* **1999**, *99*, 1665.

22 D. A. Tomalia, J. M. J. Fréchet, *J. Polym. Sci. Part A: Polym. Chem.* **2002**, *40*, 2719.

23 D. Astruc, E. Boisselier, C. Ornelas, *Chem. Rev.* **2010**, *110*, 1857.

24 T. Nakano, Y. Okamoto, *Chem. Rev.* **2001**, *101*, 4013.

25 E. Yashima, N. Ousaka, D. Taura, K. Shimomura, T. Ikai, K. Maeda, *Chem. Rev.* **2016**, *116*, 13752.

26 S. H. Gellman, *Acc. Chem. Res.* **1998**, *31*, 173.

27 D. J. Hill, M. J. Mio, R. B. Prince, T. S. Hughes, J. S. Moore, *Chem. Rev.* **2001**, *101*, 3893.

28 C. M. Goodman, S. Choi, S. Shandler, W. F. DeGrado, *Nat. Chem. Biol.* **2007**, *3*, 252.

29 G. Guichard, I. Huc, *Chem. Commun.* **2011**, *47*, 5933.

30 B. N. S. Thota, L. H. Urner, R. Haag, *Chem. Rev.* **2016**, *116*, 2079.

31 S. E. Sherman, Q. Xiao, V. Percec, *Chem. Rev.* **2017**, *117*, 6538.

32 S. Taabache, A. Bertin, *Polymer* **2017**, *9*, 280.

33 A. D. Schlüter, A. Halperin, M. Kröger, D. Vlassopoulos, G. Wegner, B. Zhang, *ACS Macro Lett.* **2014**, *3*, 991.

34 A. Zhang, L. Shu, Z. Bo, A. D. Schlüter, *Macromol. Chem. Phys.* **2003**, *204*, 328.

35 P. M. Welch, C. F. Welch, *Nano Lett.* **2006**, *6*, 1922.

36 H. Frauenrath, *Prog. Polym. Sci.* **2005**, *30*, 325.

37 B. M. Rosen, C. J. Wilson, D. A. Wilson, M. Peterca, M. R. Imam, V. Percec, *Chem. Rev.* **2009**, *109*, 6275.

38 B. Zhang, R. Wepf, K. Fischer, M. Schmidt, S. Besse, P. Lindner, B. T. King, R. Sigel, P. Schurtenberger, Y. Talmon, Y. Ding, M. Kröger, A. Halperin, A. D. Schlüter, *Angew. Chem. Int. Ed.* **2011**, *50*, 737.

39 S. Costanzo, L. F. Scherz, T. Schweizer, M. Kröger, G. Floudas, A. Dieter Schlüter, D. Vlassopoulos, *Macromolecules* **2016**, *49*, 7054.

40 F. Dutertre, K.-T. Bang, B. Loppinet, I. Choi, T.-L. Choi, G. Fytas, *Macromolecules* **2016**, *49*, 2731.

41 Y. Chen, X. Xiong, *Chem. Commun.* **2010**, *46*, 5049.

42 J. G. Rudick, V. Percec, *Acc. Chem. Res.* **2008**, *41*, 1641.

43 S. S. Sheiko, B. S. Sumerlin, K. Matyjaszewski, *Prog. Polym. Sci.* **2008**, *33*, 759.

44 L. Feuz, F. A. M. Leermakers, M. Textor, O. Borisov, *Macromolecules* **2005**, *38*, 8891.

45 O. V. Borisov, E. B. Zhulina, T. M. Birshtein, *ACS Macro Lett.* **2012**, *1*, 1166.

46 I. V. Mikhailov, A. A. Darinskii, E. B. Zhulina, O. V. Borisov, F. A. M. Leermakers, *Soft Matter* **2015**, *11*, 9367.

47 I. V. Mikhaylov, A. A. Darinskii, *Polym. Sci. Ser. A* **2015**, *57*, 239.

48 O. V. Borisov, E. B. Zhulina, A. A. Polotsky, F. A. M. Leermakers, T. M. Birshtein, *Macromolecules* **2014**, *47*, 6932.

49 I. V. Mikhaylov, O. V. Borisov, A. A. Darinskii, F. A. M. Leermakers, T. M. Birshtein, *Vysokomol. Soedin. A* **2017**, *59*, 772.

50 I. V. Mikhailov, F. A. M. Leermakers, O. V. Borisov, E. B. Zhulina, A. A. Darinskii, T. M. Birshtein, *Macromolecules* **2018**, *51*, 3315.

51 S. Mavila, O. Eivgi, I. Berkovich, N. G. Lemcoff, *Chem. Rev.* **2016**, *116*, 878.

52 C. K. Lyon, A. Prasher, A. M. Hanlon, B. T. Tuten, C. A. Tooley, P. G. Frank, E. B. Berda, A. M. Nystroem, C. J. Hawker, J. Pyun, *Polym. Chem.* **2015**, *6*, 181.

53 M. Huo, N. Wang, T. Fang, M. Sun, Y. Wei, J. Yuan, *Polymer* **2015**, *66*, A11.

54 M. Seo, B. J. Beck, J. M. J. Paulusse, C. J. Hawker, S. Y. Kim, *Macromolecules* **2008**, *41*, 6413.

55 O. Altintas, T. Rudolph, C. Barner-Kowollik, *J. Polym. Sci., Part A: Polym. Chem.* **2011**, *49*, 2566.

56 O. Altintas, P. Gerstel, N. Dingenouts, C. Barner-Kowollik, *Chem. Commun.* **2010**, *46*, 6291.

57 O. Altintas, E. Lejeune, P. Gerstel, C. Barner-Kowollik, *Polym. Chem.* **2012**, *3*, 640.

58 O. Altintas, P. Krolla-Sidenstein, H. Gliemann, C. Barner-Kowollik, *Macromolecules* **2014**, *47*, 5877.

59 J. Romulus, M. Weck, *Macromol. Rapid Commun.* **2013**, *34*, 1518.

60 F. Wang, H. Pu, M. Jin, H. Pan, Z. Chang, D. Wan, J. Du, *J. Polym. Sci. Part A: Polym. Chem.* **2015**, *53*, 1832.

61 C.-C. Cheng, F.-C. Chang, H.-C. Yen, D.-J. Lee, C.-W. Chiu, Z. Xin, *ACS Macro Lett.* **2015**, *4*, 1184.

62 P. J. M. Stals, M. A. J. Gillissen, R. Nicolaÿ, A. R. A. Palmans, E. W. Meijer, *Polym. Chem.* **2013**, *4*, 2584.

63 S. Cantekin, T. F. A. de Greef, A. R. A. Palmans, *Chem. Soc. Rev.* **2012**, *41*, 6125.

64 T. Mes, R. van der Weegen, A. R. A. Palmans, E. W. Meijer, *Angew. Chem. Int. Ed.* **2011**, *50*, 5085.

65 N. Hosono, A. R. A. Palmans, E. W. Meijer, *Chem. Commun.* **2014**, *50*, 7990.

66 K. Matsumoto, T. Terashima, T. Sugita, M. Takenaka, M. Sawamoto, *Macromolecules* **2016**, *49*, 7917.

67 M. A. J. Gillissen, T. Terashima, E. W. Meijer, A. R. A. Palmans, I. K. Voets, *Macromolecules* **2013**, *46*, 4120.

68 P. J. M. Stals, M. A. J. Gillissen, T. F. E. Paffen, T. F. A. de Greef, P. Lindner, E. W. Meijer, A. R. A. Palmans, I. K. Voets, *Macromolecules* **2014**, *47*, 2947.

69 G. M. Ter Huurne, L. N. J. De Windt, Y. Liu, E. W. Meijer, I. K. Voets, A. R. A. Palmans, *Macromolecules* **2017**, *50*, 8562.

70 J. N. Israelachvili, D. J. Mitchell, B. W. Ninham, *J. Chem. Soc. Faraday Trans. 2: Mol. Chem. Phys.* **1976**, *72*, 1525.

71 T. Terashima, T. Sugita, K. Fukae, M. Sawamoto, *Macromolecules* **2014**, *47*, 589.

72 Y. Hirai, T. Terashima, M. Takenaka, M. Sawamoto, *Macromolecules* **2016**, *49*, 5084.

73 M. Wyszogrodzka, R. Haag, *Chem. A Eur. J.* **2008**, *14*, 9202.

74 M. Kumari, A. K. Singh, S. Kumar, K. Achazi, S. Gupta, R. Haag, S. K. Sharma, *Polym. Adv. Technol.* **2014**, *25*, 1208.

75 H. Frey, R. Haag, *Rev. Mol. Biotechnol.* **2002**, *90*, 257.

76 M. Kumari, S. Gupta, K. Achazi, C. Böttcher, J. Khandare, S. K. Sharma, R. Haag, *Macromol. Rapid Commun.* **2015**, *36*, 254.

77 A. Desai, N. Atkinson, F. Rivera, W. Devonport, I. Rees, S. E. Branz, C. J. Hawker, *J. Polym. Sci. Part A: Polym. Chem.* **2000**, *38*, 1033.

78 M. Eberhardt, R. Mruk, R. Zentel, P. Théato, *Eur. Polym. J.* **2005**, *41*, 1569.

79 Y. Liu, T. Pauloehrl, S. I. Presolski, L. Albertazzi, A. R. A. Palmans, E. W. Meijer, *J. Am. Chem. Soc.* **2015**, *137*, 13096.

80 H. Yamamoto, A. Hashidzume, Y. Morishima, *Polym. J.* **2000**, *32*, 745.

81 H. Benoit, *C. R. Phys.* **1957**, *245*, 2244.

82 B. Hammouda, *Adv. Polym. Sci.* **1993**, *106*, 87.

83 S. Förster, I. Neubert, A. D. Schlüter, P. Lindner, *Macromolecules* **1999**, *32*, 4043.

84 M. M. J. Smulders, T. Buffeteau, D. Cavagnat, M. Wolffs, A. P. H. J. Schenning, E. W. Meijer, *Chirality* **2008**, *20*, 1016.

85 G. M. Ter Huurne, M. A. J. Gillissen, A. R. A. Palmans, I. K. Voets, E. W. Meijer, *Macromolecules* **2015**, *48*, 3949.

86 X. Lou, R. P. M. Lafleur, C. M. A. Leenders, S. M. C. Schoenmakers, N. M. Matsumoto, M. B. Baker, J. L. J. Van Dongen, A. R. A. Palmans, E. W. Meijer, *Nat. Commun.* **2017**, *8*, 15420.

87 S. Imai, Y. Hirai, C. Nagao, M. Sawamoto, T. Terashima, *Macromolecules* **2018**, *51*, 398.